

Materials Horizons

Accepted Manuscript

This article can be cited before page numbers have been issued, to do this please use: Y. Yao, E. He, H. Xu, Y. Liu, Y. Wei and Y. Ji, *Mater. Horiz.*, 2023, DOI: 10.1039/D3MH00184A.



This is an Accepted Manuscript, which has been through the Royal Society of Chemistry peer review process and has been accepted for publication.

Accepted Manuscripts are published online shortly after acceptance, before technical editing, formatting and proof reading. Using this free service, authors can make their results available to the community, in citable form, before we publish the edited article. We will replace this Accepted Manuscript with the edited and formatted Advance Article as soon as it is available.

You can find more information about Accepted Manuscripts in the [Information for Authors](#).

Please note that technical editing may introduce minor changes to the text and/or graphics, which may alter content. The journal's standard [Terms & Conditions](#) and the [Ethical guidelines](#) still apply. In no event shall the Royal Society of Chemistry be held responsible for any errors or omissions in this Accepted Manuscript or any consequences arising from the use of any information it contains.

New concepts

Vitrimers are covalently cross-linked polymer networks that can be reprocessed due to the topology arrangement based on associative exchange reactions. The reprocessing including reshaping usually is done above the topology freezing transition temperature (T_v) as the exchange reactions are inactive below this temperature. The work here shows that liquid crystal (LC) vitrimers behave differently from common vitrimers. The self-assembly of liquid crystal mesogens enables the reshaping of LC vitrimers below the measured T_v . The exchange reaction is still active at temperatures below the measured T_v . When reprocessing LC vitrimers into actuators at low temperatures, the large internal contraction force at high temperatures is greatly reduced, making it possible to produce LC actuators with large sizes and batch fabrication of small actuators. The work here also indicates that the currently available methods to characterize T_v are not enough for special vitrimers like LC vitrimers.

COMMUNICATION

Received 00th January 20xx,

Accepted 00th January 20xx

DOI: 10.1039/x0xx00000x

Fabricating Liquid Crystal Vitriimer Actuators far Below the Normal Processing Temperature

Yanjin Yao^[a], Enjian He^[a], Hongtu Xu^[a], Yawen Liu^[a], Yen Wei^{[a] [b]} & Yan Ji*^[a]

Abstract: Liquid crystal vitrimers can reprocess, reshape, weld, and heal due to the exchange reaction enabled topology change despite the fully covalently cross-linked network structures. Fabricating liquid crystal (LC) vitriimer actuators is invariably done above a characteristic temperature called the topology freezing transition temperature (T_v). The reason is that it is well known that all the exchange reaction-based operations have to be performed above T_v as the exchange reaction is insignificant below T_v . Here we find that LC vitrimers can be reshaped at temperatures below the measured T_v while non-LC vitrimers cannot. The work here not only makes it possible to make reprogrammable and stable LC vitriimer actuators at low temperatures but also reminds us that both our measurement and understanding of T_v need further attention to facilitate the utilization of vitrimers in various areas.

Introduction

The interest in liquid crystal elastomers (LCEs) is rapidly increasing driven by their potential application in a wide range of areas as diverse as soft robotics¹, photonic devices², biomimetics³, tissue engineering⁴,

artificial muscles⁵, and smart textiles⁶, to name a few. One of the most extraordinary properties of LCEs is their ability to transform different kinds of stimuli into mechanical actuation⁷. The actuation originates from the LC-to-isotropic phase transition and depends on the alignment of the material. Those LCEs with uniform macroscopic alignment are called monodomain LCEs⁸, which are capable of reversible shape changes. Their counterparts without macroscopic orientation are regarded as polydomain LCEs⁹. The introduction of the vitriimer concept into LCEs not only makes it flexible to make 3D LCE actuators with various chemical compositions but also brings to LCEs new exciting features such as reprocessing, welding, healing, and reshaping¹⁰⁻¹⁴. Vitrimers are covalently cross-linked polymer networks whose emergence represents an important milestone in polymer science. Classical polymers are divided into thermosets and thermoplastics. Liquid crystalline elastomers usually are fully covalently cross-linked and belong to thermosets. Thermosets can not melt or dissolve. As a result, they can not be reprocessed while thermoplastics can. Vitrimers are distinct from both thermosets and thermoplastics. They can flow upon

^aThe Key Laboratory of Bioorganic Phosphorus Chemistry & Chemical Biology, Department of Chemistry, Tsinghua University, E-mail: jjiyan@mail.tsinghua.edu.cn

^bDepartment of Chemistry, Center for Nanotechnology and Institute of Biomedical Technology, Beijing 100084, China, Chung-Yuan Christian University, Chung-Li 32023, Taiwan, China

† Supporting information for this article is given via a link at the end of the document.

heating due to the shuffle of chemical bonds induced by exchange reactions, but they can not melt or be soluble¹⁵. Up to now, various types of LCEs vitrimers have been designed and synthesized based on different exchange reactions^{16, 17 18, 19}.

So far, fabricating LC vitrimer actuators, as well as all the recycling, reshaping, welding, and healing, has to be done above a certain temperature called the topology freezing transition temperature (T_v)²⁰. T_v usually corresponds to the temperature at which the transition from viscoelastic solid to viscoelastic liquid occurs. Below T_v , the exchange reactions are negligible, therefore vitrimers behave like traditional thermosets that can not flow; above T_v , the exchange reaction is greatly accelerated and the topology can be changed under external force²¹. For common vitrimers, both high T_v and low T_v have their pros and cons. For example, high T_v means that the material has higher thermal stability under external force and high resistance to creep. This is essential for vitrimers used as structural materials. Low T_v is good to reduce the processing temperature. For LC vitrimers, high T_v is normally preferred to ensure that there is enough gap between the isotropic-liquid crystal phase transition temperatures (T_i) and T_v , otherwise, the material has not enough thermal stability and resistance to creep.

High T_v poses a big curb on fabricating LC vitrimers. A vital issue is that the material is prone to fracture at a very small strain at high temperatures. To make monodomain LC actuators, LC vitrimers have to be stretched first. At a temperature above T_i , a large internal contraction force appears. Making actuators by reshaping at high temperatures has a big problem when applied to LC vitrimers with large sizes, as the material has a much higher contraction force than the small ones at high temperatures above T_i . Such contraction makes the sample easy to slip out of the holders which is necessary to keep the sample in the stretched state with good alignment. If the applied force of the holders on the material is too strong, the material is very easy to break at the clipped areas before being reshaped. In addition to small breaking strain at high temperatures, oxidation and degradation are other problems, which prevent repeated reprogramming many times. One important strategy to get thermal stable LC vitrimer actuators is to decrease the exchange reaction rate at high temperatures. Once the exchange rate is decreased, the processing time has to be extended from minutes to hours²². Thus, oxidation becomes even more severe. If reshaping can

be done at a relatively low temperature, then, those problems may be solved. However, it is widely accepted that reshaping needs the flow which is not possible below T_v .

To find out how low the reshaping temperature can be, we unexpectedly found that our liquid crystal vitrimers could be reshaped with an acceptable time scale at a temperature much lower than the measured T_v . There is no noticeable color change due to oxidation. Under the same condition, the non-LC vitrimer with a similar molecular structure can not be reshaped below the measured T_v , which is consistent with the usual comprehension of T_v . In our experiment, even though the LC vitrimers are easier to reshape at low temperatures compared to a non-LC vitrimer, the non-LC vitrimer has faster stress relaxation rate at high temperatures. The comparison between these LC vitrimers and their non-LC analogous indicates that maybe the self-assembly of mesons plays some kind of role in the fast exchange reaction at low temperatures. Such low-temperature processing also makes it possible to make actuators with large sizes and facilitate the batch production of actuators. The reshaping at low temperatures clearly shows that the transesterification reaction occurs at temperatures below the measured T_v . Apparently, the currently available characterization methods are far from enough and even the definition of T_v in special systems may need further discussion.

Results and Discussion

Synthesis and Characterization of vitrimers.

LC vitrimers belong to liquid crystal elastomers with exchangeable links (xLCEs)¹². We used two typical LC vitrimers: xLCE-BP and xLCE-DHMS. The chemical structures are the same as we previously reported^{13, 23} (Fig. 1a). xLCE-BP is obtained by the reaction of diglycidyl ether of 4,4'-dihydroxybiphenyl and sebacic acid. xLCE-DHMS is obtained by the reaction between 4,4'-dihydroxy-methylstilbene and sebacic acid. To ensure good actuation stability, the catalysis triazabicyclodecene (TBD) in LC vitrimers was kept at 0.25% mole ratios to the carboxyl group. The stoichiometry of carboxyl and epoxy groups was 1: 1.

As a control, we synthesized a non-LC vitrimer (Vitrimer-BA) in Fig. 1a. Vitrimer-BA is obtained by reacting diglycidyl ether of bisphenol A and sebacic acid. The synthesis followed the protocols described in our earlier publication²⁴. The details about the

synthesis can be found in the Methods. Both Fourier transform infrared (FTIR) spectra (Fig S1) and swelling experiments (Fig S2) proved that the materials were fully cross-linked. All three materials with high TBD content (e.g. 5%) were previously reported as typical vitrimers¹³. The underlying mechanism for the vitrimer feature is transesterification²⁵. At low temperatures, the transesterification is negligible. It is regarded that the transesterification is activated above the T_v . Under external force, the topology changes as an ester group and a hydroxyl group react with each other, generating a new ester and a new hydroxyl group. The new hydroxyl and ester continue to react with other hydroxyl or ester groups to produce other hydroxyl and ester groups. This process goes on until a dynamic equilibrium of the reaction is established.²⁶ TBD is a catalyst for transesterification. Here, the catalyst content is rather low, but we used to verify using xLCE-DHMS that such low catalyst content still makes the material a vitrimer even though the transesterification rate is largely reduced. We also found that all the

vitrimers here could be reshaped at 180 °C for 2 hours despite that the exchange reaction is slower than that with high TBD content. Differential scanning calorimetry (DSC) (Fig. 1b) shows that the T_i for xLCE-BP and xLCE-DHMS are 120 °C and 89 °C upon heating, while the glass transition temperature (T_g) is 60 °C for the former and 42 °C for the latter. For Vitrimer-BA with 0.25% TBD, it has a T_g at 32 °C. The as-prepared LC vitrimers are unoriented polydomain LCE. 2D XRD displays two uniform rings, which is typical of an unoriented smectic sample (Fig. 1c). The inner ring corresponds to the distance between smectic layers while the outer ring corresponds to the lateral spacing between the mesogen. For xLCE-BP, the distance between smectic layers is 14.5 Å while the spacing between mesogen is 4.3 Å. For xLCE-DHMS, the former also is 16.0 Å and the latter is 4.4 Å. In the smectic phase, the rod-like liquid crystal mesogens form a layered structure while the flexible chains containing ester and hydroxyl groups stay between the layers, accounting for the fluidity of the networks (Fig. 1d).

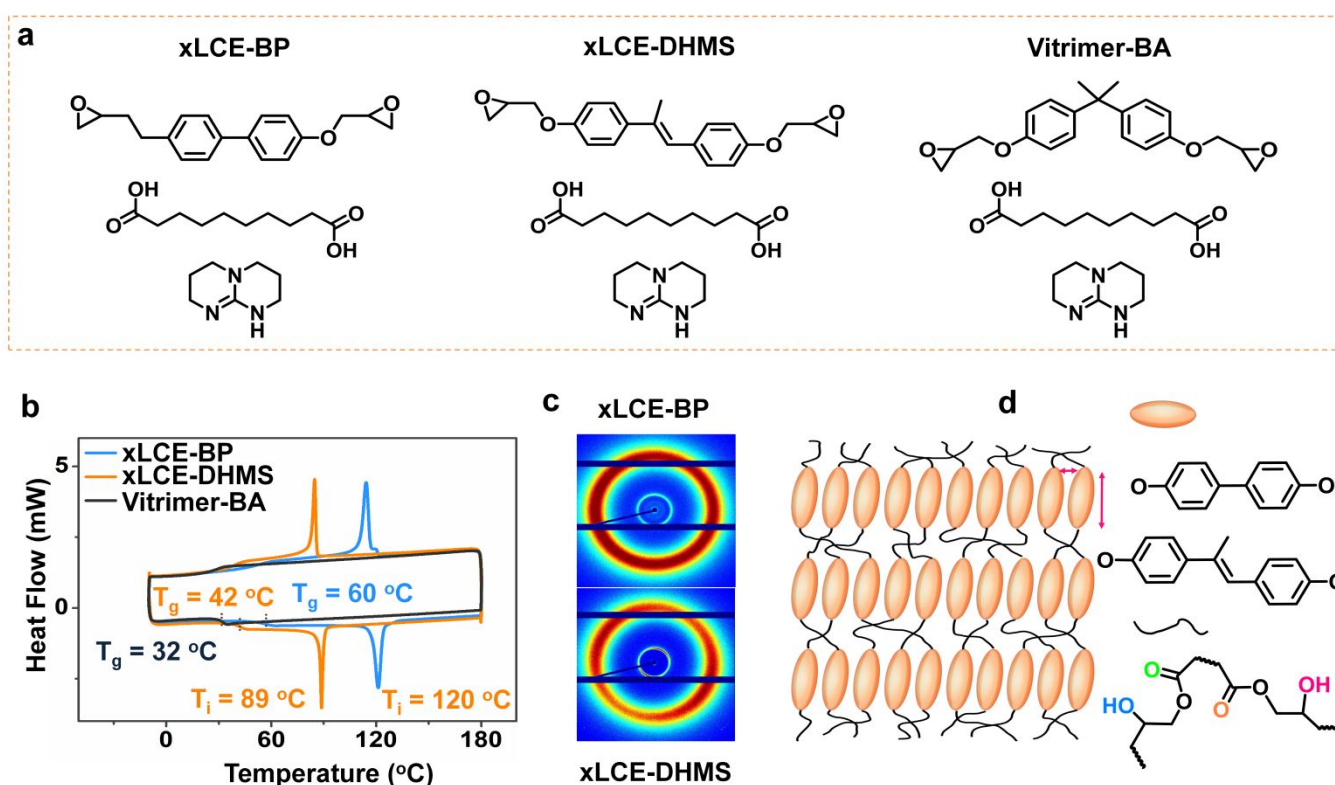


Fig. 1 Synthesis and characterization of vitrimers. (a) Chemicals for the synthesis of vitrimers. (b) DSC tests of vitrimers (both the heating and cooling rate were 5 °C/min). (c) The X-ray images of the polydomain xLCE-BP and xLCE-DHMS (d) Illustration of the microstructure of smectic-A liquid crystals.

COMMUNICATION

The elongation at break at high temperatures and that at low temperatures are quite different. Representative stress-strain curves are shown in Fig. 2a. In the experiment condition, the strain at break is 14% for xLCE-BP, 16% for xLCE-DHMS, and 6% for Vitrimer-BA at 180 °C. The strain at break increases substantially when the temperature decreases. At 80 °C, both LC vitrimers exhibit a broad soft elastic

plateau²⁷ and high strain at break (335% for xLCE-BP and 307% for xLCE-DHMS). A more detailed investigation of the tensile experiment at different temperatures was summarized in Fig. 2b. At 180 °C, the oxidation is quite obvious after two hours as the color of samples has changed, while vitrimers remain the same optical appearance as the original one after several days at lower temperatures (Fig. 2c).

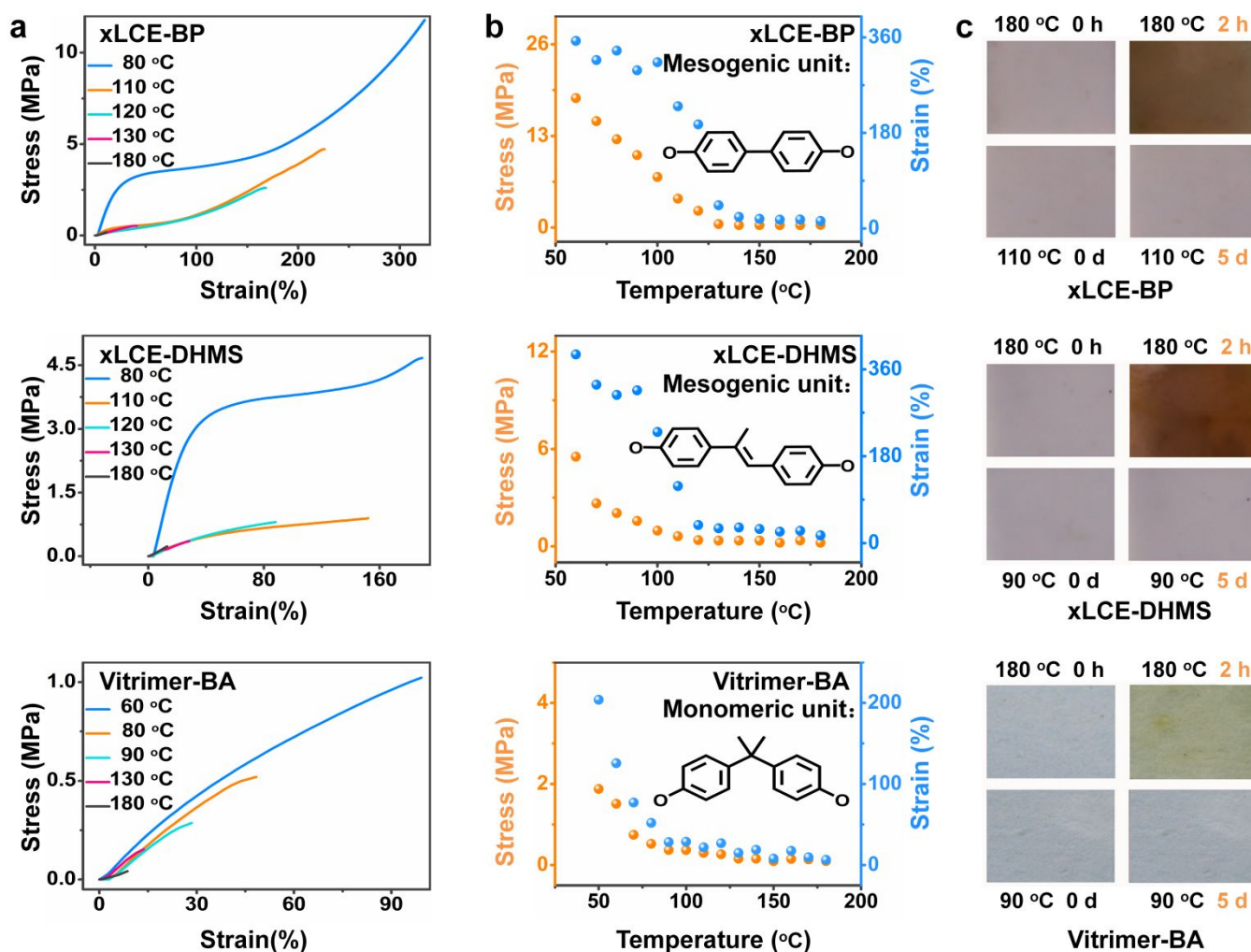


Fig. 2 Tensile tests and oxidation experiments at different temperatures for three vitrimers, respectively. (a) Characteristic stress-strain curves of the xLCE-BP, xLCE-DHMS, and Vitrimer-BA at different temperatures. (b) Changes of maximum elongation at break and corresponding stress at different temperatures for three vitrimers. (c) Optical image of three vitrimers after being placed in 180 °C air atmosphere for 2 hours (h) and low-temperature in air atmosphere for 5 days (d) respectively.

COMMUNICATION

Measurement of T_v

We measured the T_v by shear stress relaxation experiment²⁰. Up to now, there are different methods to measure T_v ²⁸. When we compared the results of the previous epoxy vitrimer obtained by reacting diglycidyl ether of bisphenol A with adipic acid and containing 5 mol% TBD, we found that T_v values measured by dilatometry, AIE luminogens, and shear stress relaxation experiment are 160 °C²⁹, 102 °C³⁰ and 62 °C³¹, respectively. The stress relaxation experiment gives out the lowest T_v . Meanwhile, for the T_v measured by shear stress relaxation experiment, T_v is denoted as the point at which the viscosity reaches 10^{12} Pa·s (the liquid-to-solid transition viscosity), below which the material no longer flows. T_v is quite like T_g . Below T_g , the polymer segmental mobility is considered to be "frozen". For vitrimers, the network topology is "frozen" below T_v . Inherited from the definition of T_g in molecular systems, T_v is usually defined as the temperature at which (extrapolated) viscosity reaches 10^{12} Pa·s. T_v is also highly dependent on the time frame that is relevant to the experiment. This is similar to T_g when measured by DSC as different scan rate gives out a different T_g . Also, like T_g , the value of T_v can be very different when using different characterization method. T_v is not a binary situation, but a spectrum³⁰. Treating T_v as an absolute value can be misleading. However, the measurement of T_v is still useful for the characterization of vitrimers, which can not only help us to set the reprocessing temperature but also to understand the relaxation in vitrimers. Therefore, we used shear stress relaxation experiment here to measure the T_v of all three vitrimers as all the other kind of methods only give out even higher T_v .

For all the samples, experiments were all done with an applied strain γ of 1%. The relaxation of the three vitrimers at different temperatures was measured. The amount of time that the samples need to relax to 37% (1/e) of the initial stress is utilized as characteristic relaxation times τ^* . Viscosity is related linearly to τ^* . All materials relax faster at higher temperatures. For example, as shown in Fig. 3a, τ^* for xLCE-BP decreases from 55298 s at 180 °C to 6778 s at 240 °C. At 180 °C, τ^* values of xLCE-BP, xLCE-DHMS, and Vitrimer-BA are 55298 s, 48062 s, 25322 s, respectively. Therefore, the LC vitrimers have a slower relaxation at high temperatures compared with the non-LC vitrimer, indicating that the non-LC vitrimer is easier to be processed than the LC vitrimers at high temperatures.

As expected, even though the catalyst content is very low, the relaxation times τ^* still follow an Arrhenius law at high temperatures as proved by the linear correlation of $\ln(\tau)$ with $1000/T$. The activation energy for viscous flow (E_a) can be calculated from the slope of the Arrhenius plot. Even though the exchange reaction for all those three materials is the same, the E_a of the three vitrimers is quite different. Both LC vitrimers have a lower activation energy than non-LC vitrimer. T_v values were determined by calculating the viscosity from τ^* and extrapolating to the point where it corresponds to 10^{12} Pa·s, as previously reported³² (the details can be found in the Methods). As shown in Fig. 3b, the values of T_v for xLCE-BP, xLCE-DHMS, and Vitrimer-BA with 0.25% TBD are 115 °C, 127 °C, and 113 °C, respectively.

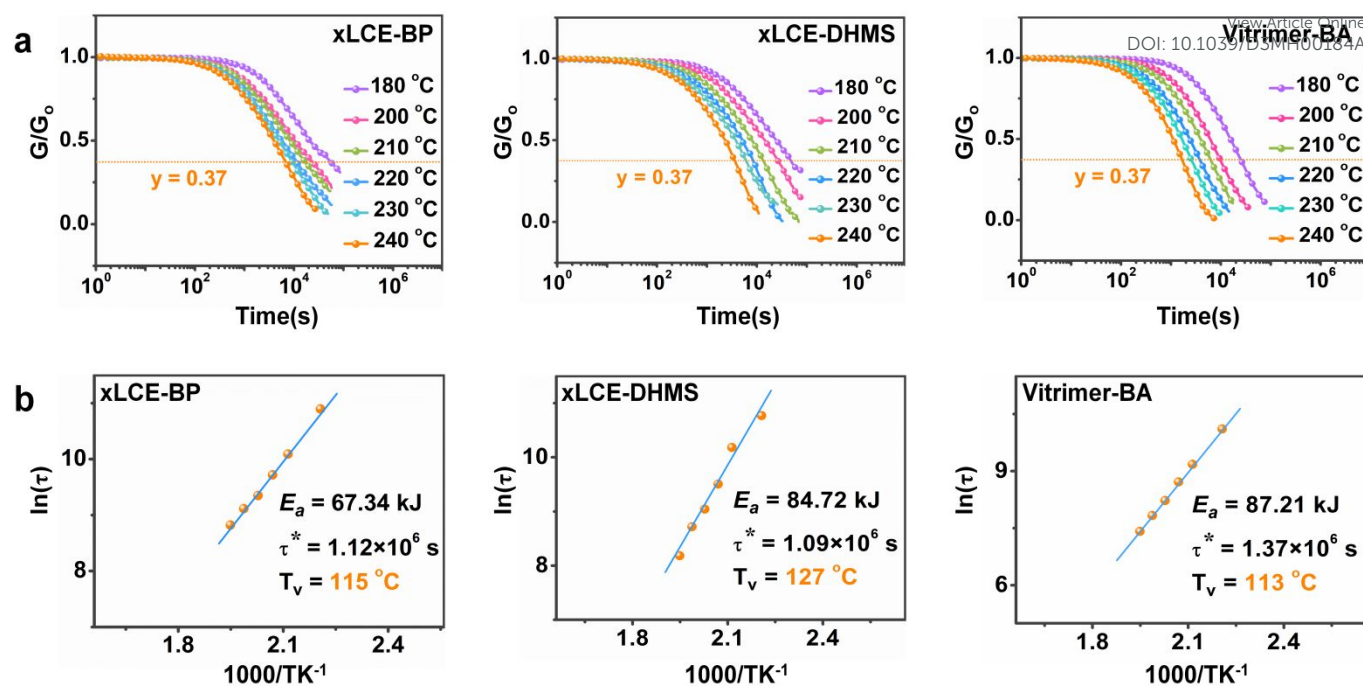


Fig. 3 (a) Stress relaxation curves of the vitrimers at varying temperatures. (b) Arrhenius plot of the measured relaxation times for the vitrimers

Reshaping at low temperatures

We found that LC vitrimers can be reshaped at temperatures below the measured T_v , while the non-LC vitrimer has to be reshaped above the measured T_v . As shown in Fig. 4a, xLCE-BP, xLCE-DHMS, and Vitrimer-BA were reshaped by folding with samples of the same sample size and at the same temperatures for 24 hours while maintaining the same external force. Afterward, the external force was removed. The films were heated to 150 °C (a temperature high the T_i of both LC vitrimers) and cooled down to remove the elastic deformation. There is no plastic deformation of Vitrimer-BA when reshaped at 90 °C and 100 °C, and only slight deformation at 120 °C. Large plastic deformation is visible only at 140 °C. The measured T_v of Vitrimer-BA is around 113 °C. Therefore, the result here is consistent with the usual comprehension that it is hard to reshape below T_v .

Different from Vitrimer-BA, xLCE-BP and xLCE-DHMS have obvious plastic deformation at 90 °C. Both LC vitrimers were converted into bend shapes after the elastic deformation was removed at 150 °C and cooling down. The bends became flat when heated to above T_i as the local alignment in the film led to actuation upon LC-isotropic phase transition. When cooled down, the

bends reformed. As the reshaping temperature increased, the final bend angle decreased. Meanwhile, xLCE-DHMS turned yellow at 140 °C, which also shows that low temperature processing is very important to avoid the oxidation of materials.

The plastic deformation means that transesterification reaction occurs in the LC vitrimer even when the reshaping temperature is below the measured T_v . The formation of the bend is not a shape memory effect of smectic LCEs³³. New shapes formed by the shape memory effect of LCEs are temporary shapes. Once heated to a temperature higher than T_i , those shapes would disappear. In the above reshaping experiment, the bends formed under T_v and those formed above T_v have the same thermal stability. They do not disappear when heated to above T_i and cooled down. Therefore, transesterification occurs in the LC vitrimers when the temperature is lower than T_v . By comparison, for the non-LC vitrimer, no permanent bend can form when the temperature is lower than its T_v , indicating a much lower transesterification rate compared to LC vitrimers. External force indeed has a great effect on the exchange reaction, but the external force here for the three samples is the same. So, the external force is not

the major reason accounting for the direct reshaping of LC vitrimers here. Even though any slow exchange reaction can lead to significant topology change if time is long enough according to the time-temperature equivalent principle, for the same time we used here, the non-LC vitrimer (Vitrimer-BA) can not be reshaped. For Vitrimer-BA and xLCE-BP, their T_v values are very close while the reshaping at 90 °C and 100 °C of them is quite different.

The transesterification reaction does not stop in the LC vitrimer when the temperature is under the measured T_v . This gives rise to the question how to define T_v in LC vitrimers. The T_v obtained in stress relaxation experiment is obtained by extrapolating the data at high temperatures. This extrapolation also relies on the fundamental assumption that the viscosity will continue to show the same temperature dependency. According to the above stress relaxation experiments, the Vitrimer-BA relaxes much faster than the LC vitrimers at high temperatures, while the reshaping experiment shows that the transesterification is faster in LC vitrimers than in Vitrimer-BA. Therefore, the actual viscosity profile of LC vitrimers should not be in line with the above assumption.

In LC vitrimers, the assembly of the mesogens lead to micro/nano-phase separation. Phase separation was an important reason for the very fast stress relaxation in vitrimers as the soluble fraction of the materials acting as a plasticizer³⁴. In the absence of a plasticizer, block copolymer vitrimers display resistance to macroscopic deformation as the microphase-separated network structure adds constraints on the network diffusion^{35, 36}. Such phase segregation can be used to tune the thermal and mechanical properties of vitrimers³⁷. Theoretical work shows that relaxation times are much lower in gradient and blocky vitrimers³². Evidence has been found that micro-phase separation can increase the network connectivity defects³⁸, which will facilitate stress relaxation³⁹. In another report, a self-associated alkyl chain coupled with the exchange reaction led to fast stress relaxation rates⁴⁰. However, none of the previous works ever investigate whether the reshaping can be done below T_v .

View Article Online
DOI: 10.1039/D3MH00184A

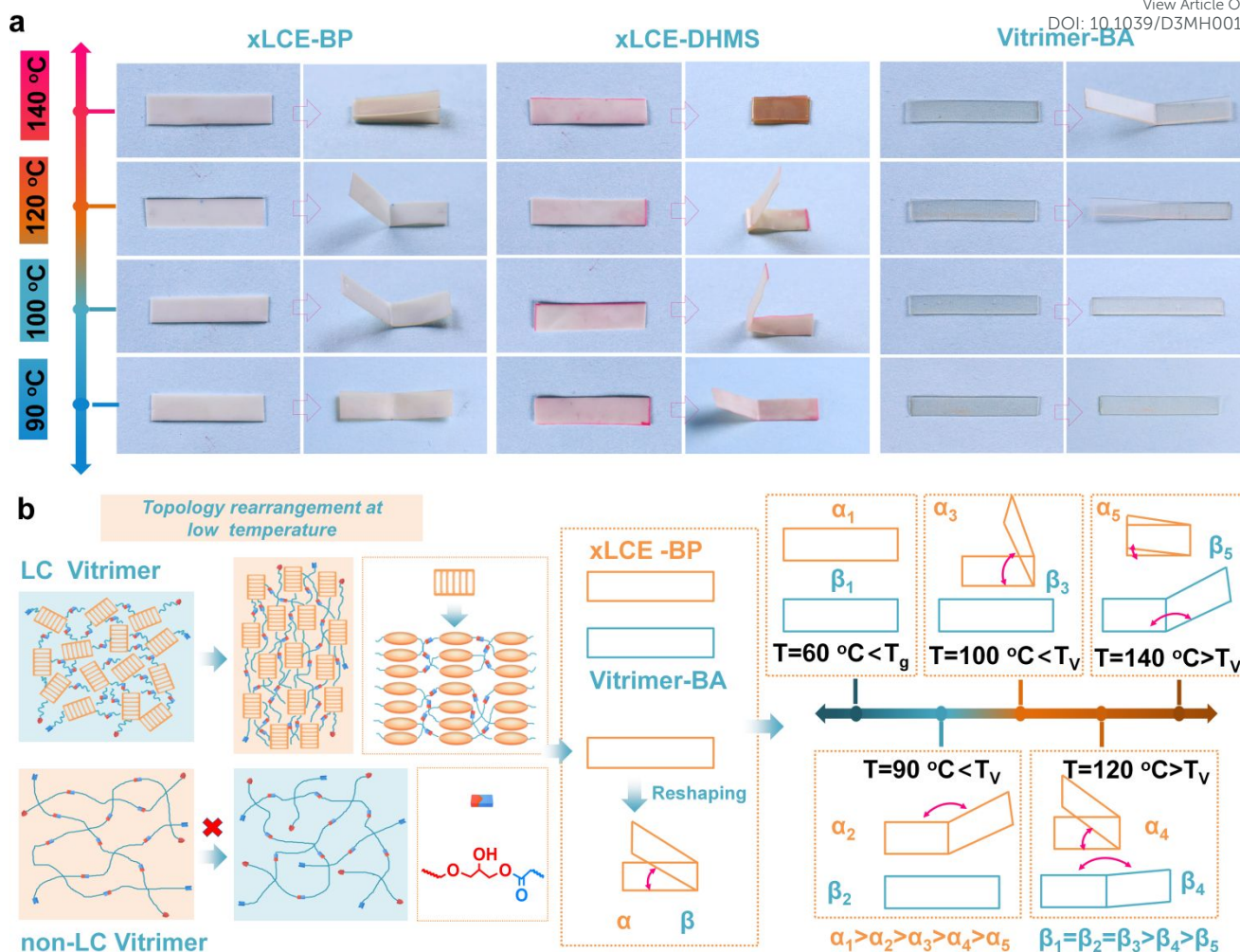


Fig. 4 (a) Reshaping of xLCE-BP, xLCE-DHMS, and Vitrimer-BA at different temperatures. (b) Illustration on the difference between the microstructure and the reshaping results between an LC vitrimer and a non-LC vitrimer. For the LC vitrimer, the assembly of mesogens leads to local aggregation of ester and hydroxyl groups while no such structure exists in the non-LC vitrimer. Therefore, the xLCE-BP can be reshaped and the bend angle decreases as the reshaping temperature increases, even though the reshaping temperature is lower than its T_v . On the contrary, non-LC vitrimer (Vitrimer-BA) can only be reshaped at a temperature above T_v . As the temperature increases, the bending angle of xLCE-BP (α) decreases while the bending angle of Vitrimer-BA (β) remains 180° below T_v and only decreases after the temperature is above T_v .

We suppose that the reason that the LC vitrimers can be reshaped at low temperatures may relate to the self-assembly of liquid crystal mesogens. Considering the structure of the smectic phase, the ester groups and the hydroxyl groups are confined within the domains formed by flexible segments, as illustrated in Fig. 4b. Therefore, the local concentration of the ester groups and hydroxyl groups is much higher than that

in the layers formed by rod-like mesogens. As the exchange rate depends on the concentration of reaction groups⁴¹, it is reasonable that the exchange reaction between the mesogen layers is more active compared with the exchange reaction in non-LC vitrimer where there is no local aggregation of esters and hydroxyl groups.

Fabricating LC vitrimer actuators at low temperatures

Similar to the reshaping by folding, xLCEs can be made into monodomain materials with good macroscopic orientation, resulting in load-free actuation. For example, when a 1 cm xLCE-DHMS film is stretched to 1.5 cm and left at a 110 °C (17 °C lower than the measured T_v) oven for 24 hours, the film became 2 cm after cooling down to room temperature and the external stress was removed. This film is capable of reversible shape change when the film transforms from an isotropic phase to an LC phase. The spontaneous actuation strain reaches 100%, as shown in Fig. 5a. The alignment of LCE was confirmed by both polarized optical microscopy (POM) (Fig. 5b) and 2D X-ray diffraction (2D XRD) (Fig. 5c). Calculated from the Azimuthal scan, the value of the orientation parameter of xLCE-DHMS, S , is 0.85. Similarly, at 110 °C, an xLCE-BP film with a pre-strain of 233% can also be made into a monodomain xLCE-BP with an actuation strain of 100% and an orientation parameter of 0.83. The details were shown in Fig. S3. The processing temperature can be even lower. For example, at 80 °C for 24 hours, both xLCE-DHMS and xLCE-BP become monodomain material. But the actuation strain is 80% for xLCE-DHMS and 60% for xLCE-BP. When the heating time was extended to 3 days, both the actuation strain for xLCE-BP and the actuation strain for xLCE-DHMS can reach 100% at 80 °C.

The exchange reaction may be still active so long as the temperature is above T_g . To verify this, we tried even lower temperatures. We found that none of the three vitrimers could be reshaped at 70 °C, but when we extended the reprocessing time to 3 days, as shown in Fig. S4, xLCE-DHMS could still be perfectly made into a monodomain actuator at 70 °C (57 °C lower than the measured T_v). When the temperature reached to 60 °C (67 °C lower than the measured T_v), the actuation strain could still reach about 30% ~40%. But xLCE-BP can no longer be made into monodomain at 70 °C. According to the DSC test results, the T_g values for Vitrimer-BA, xLCE-BP, and xLCE-DHMS are 32 °C, 42 °C, and 60 °C respectively. According to dynamic mechanical analysis (DMA) (Fig. S5), the T_g values for Vitrimer-BA, xLCE-BP, and xLCE-DHMS are

40 °C, 51 °C, and 66 °C, respectively. As we previously pointed out, the glass transition is not a point but a spectrum. So, even though 70 °C is several degrees higher than the measured value, the segmental mobility of xLCE-BP is mostly frozen.

Low temperature will not only reduce failure due to high temperature-related snaps but also is suitable for fabricating LC film actuators of relatively large sizes. Here the reshaping temperature can be below T_i . As the material is in the LC phase, there is a very low force of contraction force, which means that the problems caused by the contraction force due to the alignment will be greatly reduced. As shown in Fig. S6, we can get a monodomain LCE with a size of 10 cm*16 cm. Such size is limited by our ability to make big original xLCE films. If one can make a bigger film, the size can be enlarged easily.

Low-temperature processing is also suitable for LC vitrimers with different catalyst content. We prepared vitrimers with 5 mol% of TBD. The T_v values of xLCE-BP, xLCE-DHMS, and Vitrimer-BA with 5 mol% TBD were calculated to be 85 °C, 91 °C, and 83 °C according to Fig. S7, respectively. The three vitrimers were reshaped at 60 °C for 3 days. We found that only xLCE-DHMS could be reshaped successfully, as shown in Fig. S8. As the T_g of xLCE-BP is above 60 °C, it is reasonable that it can not be reshaped. For xLCE-DHMS and Vitrimer-BA, the values of their T_g are 54 °C and 41 °C respectively, which are both below 60 °C. However, xLCE-DHMS can be reshaped while Vitrimer-BA can not. This agrees with the conclusion that reshaping of LC vitrimers can be done at temperatures lower than the measured T_v while this is not true for the non-LC vitrimer. We also tried vitrimers without catalyst. As we previously verified, transesterification reaction still exists in xLCE-BP without catalyst²². xLCE-DHMS is the same. As the higher the catalyst content, the higher the measured T_v . The T_v of those vitrimers should be higher than those with 0.25 mol% TBD. We found that reshaping of both xLCE-BP and xLCE-DHMS without catalyst could be done at 80 °C for 3d (Fig. S9). Therefore, the low temperature-processing method is also suitable for LC vitrimer without a catalyst.

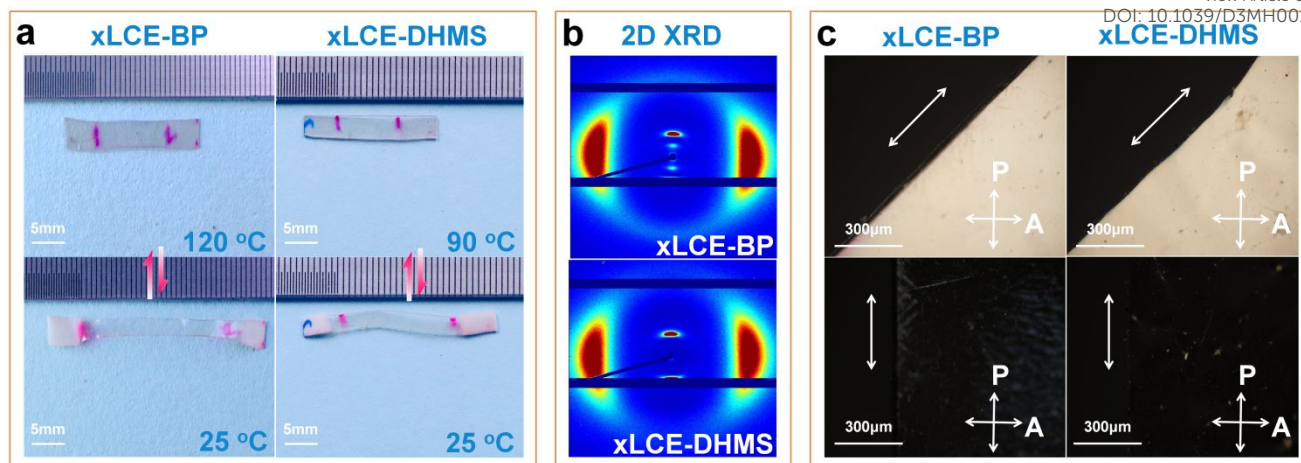


Fig. 5. Actuation and characterization of monodomain of xLCE. (a) Thermal actuation of the monodomain xLCE-BP and xLCE-DHMS processed at low temperatures. (b) 2D x-ray diffraction patterns of monodomain xLCE-BP and xLCE-DHMS. (c) POM images of monodomain for xLCE-BP and xLCE-DHMS at room temperature being rotated at the interval of 45°. Alignment of monodomain xLCE-BP and xLCE-DHMS at 25 °C ($T < T_i$) under POM crossed polarizers showing the uniaxial orientation and the birefringence.

The fabrication of 3D actuators can also benefit from low temperatures. For example, we can fabricate dome shapes using metal dies with different diameters by the method illustrated (details can be found in the Methods), and the preparation process of the dome and dome arrays were shown in Fig. 6a. As the strain at break can be significantly larger at low temperatures compared to it at high temperatures, the low-temperature process is more reliable compared with that at high temperatures. Additionally, low-temperature reprocessing is also applicable for the batch production of LC actuators. Using the above method, we can get dome arrays of different sizes (Fig. S10). The domes vanished when heated to a temperature above T_i and reappeared when cooling down to a temperature lower than the measured T_i . They can be easily controlled using electrothermal heating provided by commercial flexible polyimide (PI) heating films. Such films use nickel-chromium alloy as the conductive element laminated between two layers of Kapton films. The conductive elements can convert input voltage to thermal energy. When the voltage is applied, the temperature of the conductive PI film increases. As a

result, the dome becomes flat when the temperature reaches T_i (Fig. 6b). When the voltage is removed, the dome pops out again. As the electrothermal PI films can be easily made into desirable conductive patterns (Fig. 6b), each dome can be controlled individually. Different domes can be kept either flat or in dome shapes, resulting in different patterns similar to haptic displays⁴²⁻⁴⁴ (Fig. 6b-d). In our current device, we have to control the pattern manually. When changing a pattern, we turn the switch, the pattern becomes a new one in a minute if the dome size is 5.0 mm (diameter) \times 3.0 mm (height) (A video is provided as Video S1). The spatial resolution can be much better when a suitable mold is used. In addition, the actuation temperatures of xLCE-BP and xLCE-DHMS are far above the proper temperature range that human beings can bear. Even though the work shows the low-temperature processing here is very promising for the batch production of actuators, much more future work is necessary to make a real braille display using an xLCE with a lower T_i and with better designs to improve both the refreshing time and the spatial resolution.

COMMUNICATION

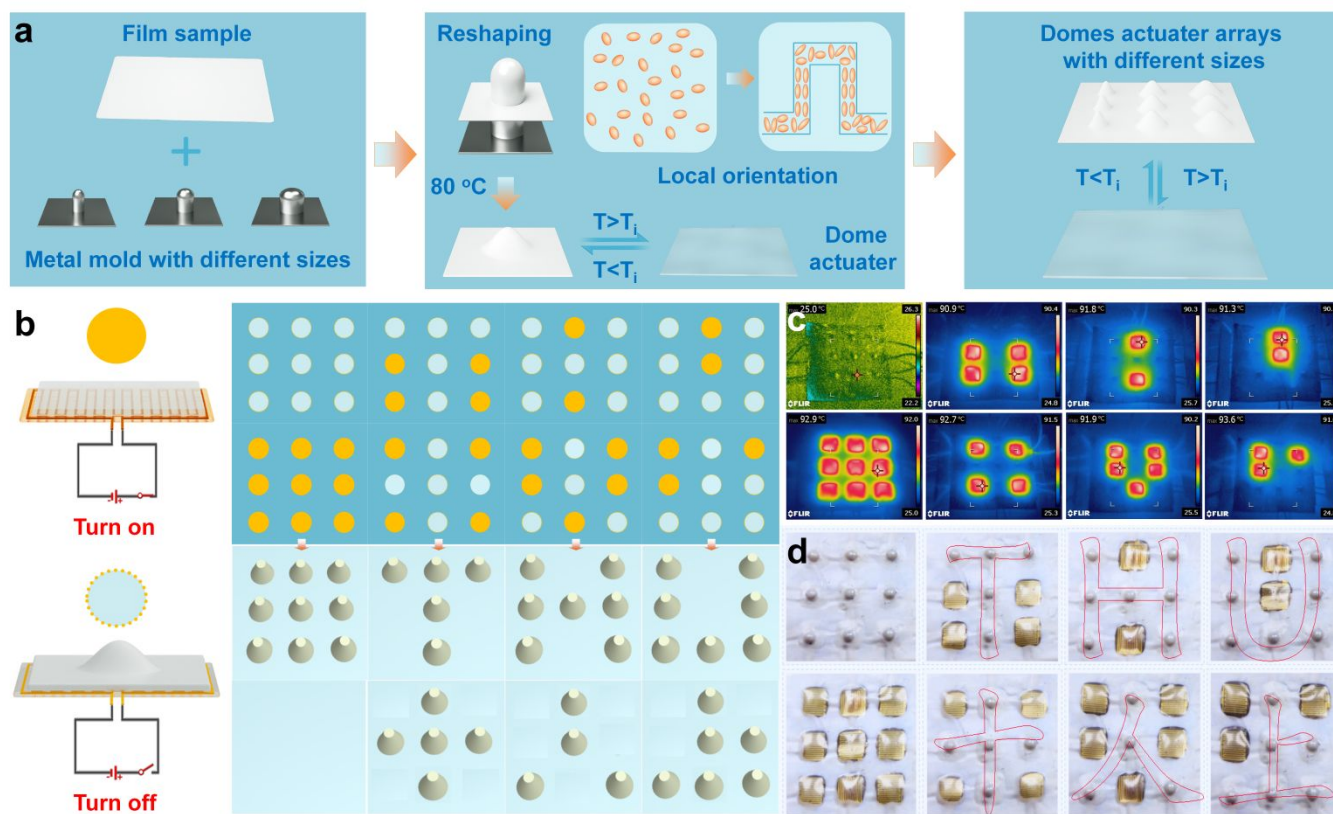


Fig 6. xLCE domes made at 80 °C. (a) Demonstration diagram of the dome and dome array preparation process. (b) Demonstration of electrically driven dome arrays. (c) The thermography of the electrically driven dome arrays. (d) The optical image of the electrically driven dome arrays.

Conclusion

In summary, the work here proved that fabricating LC vitrimer actuators can be done at a temperature much lower than the measured T_v , even though T_v is regarded as the lowest temperature for vitrimers to flow. As an alternative choice to high temperature, such low-temperature processing is more robust as the strain at break is greatly increased, which can greatly extend the flexibility of reshaping and actuator fabrication in more scenarios. Meanwhile, the oxidation of xLCEs with a low exchange reaction rate is greatly reduced as a long time at high temperatures is avoided. Fabricating LC vitrimer actuators below T_i also evades the difficulties resulting from the large contraction force at high temperatures which has to be balanced during fabrication, especially for large-size actuators. Low-temperature processing can be combined with

electrothermal films for the production of actuator arrays. The behavior of LC vitrimers and that of non-LC vitrimers were found to be quite different at low temperatures, resulting from the self-assembly of mesogens in LC vitrimers. The work here also shows that LC vitrimers provide a unique platform to further understand the intriguing structure-property relationships in vitrimers, which is crucial for the practical application of vitrimers and has started to attract more and more attention recently.

Experimental Section

Chemicals. Triazabicyclodecene (TCI, 98%), sebacic acid (TCI, 99.0%), diglycidyl ether of bisphenol A (DGE-BA) (Sigma-aldrich, D.E.R. 332), and dichloromethane (DCM) were used directly without further purification. Diglycidyl ether of 4, 4'-dihydroxy- α -methylstibene (DGE-DHMS) and diglycidyl ether of 4, 4'-dihydroxybiphenyl (DGE-BP) were synthesized following the procedure outlined in Mol. Cryst. Liq. Cryst. 266, 9 (1995)⁴⁵.

Preparation of xLCE-BP. The preparation of xLCE-BP is similar to the procedure described in our previous work.¹³ A stoichiometric amount of diglycidyl ether of 4, 4'-dihydroxybiphenyl (DGE-BP) (2.3840 g, 8 mmol) and sebacic acid (1.6160 g, 8 mmol) were mixed at 170 °C. A triazabicyclodecene catalyst (0.25 mol% to the COOH groups) was introduced and stirred manually until homogeneous. As the mixture became very viscous, it was cooled to room temperature to obtain a solid product that was not completely cross-linked. Then the solid was sandwiched between two plates to be cured by a hot press with 3 MPa pressure for 6 hours at 170 °C. xLCE-BP without catalyst and with 5 mol% TBD were synthesized using the same method except that the catalyst content is different.

Preparation of xLCE-DHMS. The preparation of xLCE-DHMS is similar to the procedure described in our previous work.²³ A stoichiometric amount of 4, 4'-dihydroxy- α -methylstibene (2.7200 g, 8 mmol) and sebacic acid (1.6160 g, 8 mmol) were mixed at 160 °C. A triazabicyclodecene catalyst (0.25 mol% to the COOH groups) was introduced and stirred manually until homogeneous. As the mixture became very viscous, it was cooled to room temperature to obtain a solid product that was not completely cross-linked. Then the solid was sandwiched between two plates to be cured by a hot press with 3 MPa pressure for 6 hours at 160 °C. xLCE-DHMS without catalyst and with 5 mol% TBD content were synthesized using the same method except the catalyst content is different.

Preparation of Vitrimer-BA. The preparation of Vitrimer-BA is similar to the procedure described in our previous work²⁴. Stoichiometric amounts of diglycidyl ether of bisphenol A (2.7200 g, 8 mmol) and sebacic acid (1.6160 g, 8 mmol) were mixed and heated to 160 °C. After the mixture was melted, triazabicyclodecene (0.25 mol% to the COOH groups) was introduced and stirred manually till homogeneous. As the mixture became very viscous, it was cooled to room temperature to obtain a solid product that was not completely cross-linked. Then the solid was sandwiched between two plates to be cured by a hot press with 3 MPa pressure for 6 hours at 160 °C. Vitrimer-BA without catalyst and with 5 mol% TBD content were synthesized using the same method except the catalyst content is different.

Swelling and Gel content tests. The swelling experiments for the polydomain xLCE (xLCE-BP and xLCE-DHMS) and Vitrimer-BA were done following the procedure below. We cut a sample with a side length of 1 cm for xLCE-BP, xLCE-

DHMS, and Vitrimer-BA respectively, then weighed them separately and recorded them as m_0 . The values of m_0 for xLCE-BP, xLCE-DHMS, and Vitrimer-BA are 0.0210 g, 0.0370 g, and 0.0333 g respectively. After weighing, they are swelled in 20 ml anhydrous DCM at room temperature for 3 days with the solvent being refreshed daily, respectively. The original size for xLCE-BP, xLCE-DHMS, and Vitrimer-BA were 10.00 mm \times 10.00 mm \times 0.17 mm, 10.00 mm \times 10.00 mm \times 0.31 mm, and 10.00 mm \times 10.00 mm \times 0.26 mm, respectively. In the swelling solvent for 3 days, the volumes of samples for three samples all reached their maximum, and their volume values don't change anymore. 12.50 mm \times 13.00 mm \times 0.24 mm for xLCE-BP, which is 2.20 times the original size in volume; 13.00 mm \times 14.00 mm \times 0.39 mm for xLCE-DHMS, which is 2.29 times the original size in volume; 15.00 mm \times 15.00 mm \times 0.34 mm for Vitrimer-BA, which is 2.94 times the original size in volume. Afterward, the residual samples were dried at 50 °C in a vacuum oven overnight until the weight of the three samples all reached a constant value of m_4 , 0.0193 g for LCE-BP, 0.0360 g for xLCE-DHMS, and 0.0308 g for Vitrimer-BA respectively. The gel content was calculated as the weight ratio of the vitrimers after and before the solvent extraction⁴⁶, the values of gel fractions are calculated as 92% for LCE-BP, 97% for xLCE-DHMS, and 93% for Vitrimer-BA respectively, which proved that the materials are all fully cross-linked (Fig. S2).

Reshaping different vitrimers at low temperatures. Films of xLCE-BP, xLCE-DHMS, and Vitrimer-BA with a length, width, and thickness of about 2 cm \times 5 mm \times 0.26 mm were folded and then sandwiched between two pieces of glass at different temperatures for 24 hours while maintaining the same external force.

Preparation of monodomain of xLCE-BP and xLCE-DHMS. The xLCE-BP and xLCE-DHMS polydomain samples were swelled in anhydrous dichloromethane for 24 hours respectively and then took them out until the volume did not change. After swelling, they were dried in an oven at 50 °C until their weights were constant. After drying, the sample was cut into a rectangle with a length, width, and thickness of about 2 cm \times 3 mm \times 0.26 mm. The samples were stretched by the desired strain of the original length at a temperature above T_g and the ends were fixed. The fixed stretched samples were heated for a desired time at 110 °C or 80 °C. Then the samples were annealed at 130 °C. Final monodomain samples were obtained after cooling down.

Fourier transform infrared (FTIR) spectra. FTIR spectra were obtained on Perkin Elmer spectrum 100, the results clearly showed that the characteristic peaks of the epoxy peak at 910 cm^{-1} disappeared after curing for 6 h, confirming the completion of the curing reactions (Fig. S1).

Tensile tests. Stress-strain curves were measured on a TA-Q800 DMA apparatus in the film-tension geometry from 50 °C to 180 °C, at intervals of 10 degrees. xLCE-BP, xLCE-DHMS, and Vitrimer-BA films individually were tested using

controlled force mode with a force rate of 0.1 N/min for xLCE-BP and xLCE-DHMS, 0.5 N/min for Vitrimer-BA. The stress-strain experiments were performed at least three times for each sample.

Differential scanning calorimetry (DSC) experiments. Differential scanning calorimetry (DSC) was performed using the TA-Q2000 DSC apparatus, the scan range ranges from -10 °C to 180 °C, and then from -10 °C to 180 °C. This process is repeated twice, the first scanning rate is 20 °C/min, the second scanning rate is 5 °C/min, and the second data is plotted.

Thermogravimetric analysis (TGA). TGA results were obtained on TA instruments Q50 under a nitrogen atmosphere with a heating rate of 10 °C min⁻¹ from room temperature to 800 °C. TGA results showed the degradation temperature of materials (Fig. S11).

Dynamic mechanical analysis (DMA). DMA results were acquired on a TA Instruments Q800 machine. DMA was used to obtain the modulus-temperature and tan δ-temperature curves of the original samples to determine their T_g and T_i, respectively. The curves were measured at 1 Hz frequency and 1 °C min⁻¹ heating rate from 20 °C to 200 °C in tension mode. T_g was determined at the maximum of the tan δ-temperature curve, while T_i was determined at the minimum of the storage modulus curve

X-ray diffraction (XRD) experiments. 2D XRD images were obtained on the Instrument of SAXSLAB Ganesha. Discover a diffractometer with a wavelength of 0.154 nm. XRD experiments were conducted to confirm the alignment of LCEs. The order parameter was calculated based on the Hermans-Stein orientation distribution function shown below in Equation 1 (eqn 1):

$$S = \frac{3 \langle \cos^2 \phi \rangle - 1}{2} \quad (\text{eqn 1})$$

$$\langle \cos^2 \phi \rangle = \frac{\int_0^{\pi} I(\phi) \sin \phi \cos^2 \phi d\phi}{\int_0^{\pi} I(\phi) \sin \phi d\phi} \quad (\text{eqn 2})$$

Where S is the order parameter, φ is the azimuthal angle, and I is the intensity as shown in Fig. S3

POM. A Nikon ECLIPSE LV100POL polarizing optical microscope equipped was used to observe the uniaxial orientation and the birefringence of the sample.

Stress relaxation test and topology freezing transition temperature (T_v) determination. According to our usual testing methods,²³ a TA-ARG2 rheometer was used for the stress relaxation experiments with the 8 mm parallel-plate geometry in a constant strain (γ = 1%) at varying temperatures. The sample was equilibrated at the target test

temperature for 2 min first. Then a constant normal force of 10 N was applied to ensure good contact. The stress relaxation was monitored over time when the stress relaxation modulus had relaxed to less than 37% (1/e) of its initial value. The stress relaxation experiments were performed at least two times for each sample. When the stress relaxation modulus reached 37% (1/e) of its initial value, it was defined as the characteristic relaxation time (τ*). lnτ* at various temperatures were then plotted versus 1000/T and fit the Arrhenius relationship in eqn 3,

$$\tau^* = \tau_0 e^{E_a/RT} \quad (\text{eqn 3})$$

where τ₀ is the characteristic relaxation time at infinite T, E_a is the activation energy of the transesterification reaction (kJ mol⁻¹), R is the universal gas constant and T is the target test temperature. And the temperature point when the viscosity reaches 10¹² Pa s⁻¹ was defined as T_v, it's also the point for transition viscosity from liquid to solid. So we can calculate lnτ* by using the Maxwell (eqn 4).

$$\eta = G\tau^* \quad (\text{eqn 4})$$

$$G = E'/(2(1 + \nu)) \quad (\text{eqn 5})$$

and the shear modulus G was estimated from the tensile modulus (E') which was measured by dynamic thermomechanical analysis (DMA, TA Q800) with the eqn 5. E' of the samples with different samples were calculated as the average modulus at a temperature varying from 120 °C to 200 °C from the modulus-temperature curves (Fig. 2a). The average plateau modulus of the samples with 0.25 mol% catalyst contents is 2.67 MPa for xLCE-BP, 2.74 MPa for xLCE-DHMS, and 2.19 MPa for Vitrimer-BA, respectively. The vitrimer is approximated as a special rubber elastomer, so the value of Poisson's ratio(ν) is 0.5, which is usually used for rubbers. The stress relaxation experiments were performed at least three times for each sample. The T_v values of vitrimers with 5 mol% TBD were calculated in the same way as the above for the vitrimers with 0.25 mol% TBD using Fig. S7.

Preparation of dome shapes. We used metal dies with different diameters (3 mm, 5 mm, and 10 mm) with a height of 5 mm. The xLCE film was heated to a temperature above T_g but lower than T_i and pressed on one die. After cooling down, a temporary column shape is formed. Then the die was replaced by a plastic pillar with the height and diameter corresponding to that of the metal die. The plastic pillar supports the temporary shape. The periphery of the column is fixed with high-temperature adhesive to prevent the plastic pillar and the column from moving. The whole set was heated to 80 °C for 3 days to ensure the best actuation performance. Afterward, the plastic pillar was removed and the film was reheated to a temperature above T_i. When

cooling down, a dome shape formed. Dome arrays are made in the same way.

Conflicts of interest

The authors declare no competing financial interest.

References

- Z. Liu, H. K. Bisoyi, Y. Huang, M. Wang, H. Yang and Q. Li, *Angew. Chem.-Int. Edit.*, 2022, **61**, e202115755.
- S.U. Kim, Y. J. Lee, J. Liu, D. S. Kim, H. Wang and S. Yang, *Nat. Mater.*, 2022, **21**, 129-129.
- H. Zeng, O. M. Wani, P. Wasylczyk, R. Kaczmarek and A. Priimagi, *Adv. Mater.*, 2017, **29**, 1701814.
- B. Gurboga, E. B. Tuncgovde and E. Kemiklioglu, *Biotechnol. Bioeng.*, 2022, **119**, 1047-1052.
- H. F. Lu, M. Wang, X. M. Chen, B.-P. Lin and H. Yang, *J. Am. Chem. Soc.*, 2019, **141**, 14364-14369.
- Y. Geng, R. Kizhakidathazhath and J. P. F. Lagerwall, *Nat. Mater.*, 2022, **21**, 1441-1447.
- E. R. Zubarev, S. A. Kuptsov, T. I. Yuranova, R. V. Talroze and H. Finkelmann, *Liq. Cryst.*, 1999, **26**, 1531-1540.
- S. V. Fridrikh and E. M. Terentjev, *Phys. Rev. E*, 1999, **60**, 1847-1857.
- A. Sanchez-Ferrer and H. Finkelmann, *Macromol. Rapid Commun.*, 2011, **32**, 309-315.
- Y. Zhang, Z. Wang, Y. Yang, Q. Chen, X. Qian, Y. Wu, H. Liang, Y. Xu, Y. Wei and Y. Ji, *Sci. Adv.*, 2020, **6**, eaay8606.
- Z. J. Wang and S. Q. Cai, *J. Mat. Chem. B*, 2020, **8**, 6610-6623.
- M. O. Saed, A. Gablier and E. M. Terentjev, *Chem. Rev.*, 2022, **122**, 4927-4945.
- Z. Q. Pei, Y. Yang, Q. M. Chen, E. M. Terentjev, Y. Wei and Y. Ji, *Nat. Mater.*, 2014, **13**, 36-41.
- Q. M. Chen, Y. Yang, Y. Wei and Y. Ji, *Acta Polymerica Sinica*, 2019, **50**, 451-468.
- M. Guerre, C. Taplan, J. M. Winne and F. E. Du Prez, *Chem. Sci.*, 2020, **11**, 4855-4870.
- J. Ma, Y. Yang, C. Valenzuela, X. Zhang, L. Wang and W. Feng, *Angew. Chem.-Int. Edit.*, 2022, **61**, e202116219.
- J. H. Lee, J. Bae, J. H. Hwang, M. Y. Choi, Y. S. Kim, S. Park, J. H. Na, D.G. Kim and S. k. Ahn, *Adv. Funct. Mater.*, 2022, **32**, 2110360.
- T. S. Hebner, M. Podgorski, S. Mavila, T. J. White and C. N. Bowman, *Angew. Chem.-Int. Edit.*, 2022, **61**, e202116522.
- L. Chen, H. K. Bisoyi, Y. Huang, S. Huang, M. Wang, H. Yang and Q. Li, *Angew. Chem.-Int. Edit.*, 2021, **60**, 16394-16398.
- M. Capelot, M. M. Unterlass, F. Tournilhac and L. Leibler, *ACS Macro Lett.*, 2012, **1**, 789-792.
- A. M. Hubbard, Y. X. Ren, D. Konkolewicz, A. Sarvestani, C. R. Picu, G. S. Kedziora, A. Roy, V. Varshney and D. Nepal, *ACS Appl. Polym. Mater.*, 2021, **3**, 1756-1766.
- Y. Yang, E. M. Terentjev, Y. Zhang, Q. Chen, Y. Zhao, Y. Wei and Y. Ji, *Angew. Chem.-Int. Edit.*, 2019, **58**, 17474-17479.
- Q. M. Chen, Y. S. Li, Y. Yang, Y. S. Xu, X. J. Qian, Y. Wei and Y. Ji, *Chem. Sci.*, 2019, **10**, 3025-3030.
- Z. Pei, Y. Yang, Q. Chen, Y. Wei and Y. Ji, *Adv. Mater.*, 2016, **28**, 156-160.
- D. Montarnal, M. Capelot, F. Tournilhac and L. Leibler, *Science*, 2011, **334**, 965-968.
- K. Urayama, R. Mashita, I. Kobayashi and T. Takigawa, *Macromolecules*, 2007, **40**, 7665-7670.
- M. Warner, P. Bladon and E. M. Terentjev, *J. Phys. II*, 1994, **4**, 93-102.
- S. Kaiser, P. Novak, M. Giebler, M. Gschwandl, P. Novak, G. Pilz, M. Morak and S. Schlögl, *Polymer*, 2020, **204**, 122804.
- Y. Yang, Z. Pei, X. Zhang, L. Tao, Y. Wei and Y. Ji, *Chem. Sci.*, 2014, **5**, 3486-3492.
- Y. Yang, S. Zhang, X. Zhang, L. Gao, Y. Wei and Y. Ji, *Nat. Commun.*, 2019, **10**, 3165.
- C. Liu and D. Wang, *Macromolecules*, 2022, **55**, 1260-1266.
- R. G. Ricarte and S. Shanbhag, *Macromolecules*, 2021, **54**, 3304-3320.
- Y. Li, C. Pruitt, O. Rios, L. Wei, M. Rock, J. K. Keum, A. G. McDonald and M. R. Kessler, *Macromolecules*, 2015, **48**, 2864-2874.
- R. G. Ricarte, F. Tournilhac and L. Leibler, *Macromolecules*, 2019, **52**, 432-443.
- R. G. Ricarte, F. Tournilhac, M. Cloitre and L. Leibler, *Macromolecules*, 2020, **53**, 1852-1866.
- J. J. Lessard, G. M. Scheutz, S. H. Sung, K. A. Lantz, T. H. Epps and B. S. Sumerlin, *J. Am. Chem. Soc.*, 2020, **142**, 283-289.
- Ishibashi J, Fang Y, Kalow J. Exploiting block copolymer phase segregation to tune vitrimer properties. ChemRxiv. Preprint at <https://doi.org/10.26434/chemrxiv.10000232.v3> (2019).
- J. S. A. Ishibashi, I. C. Pierce, A. B. Chang, A. Zografos, B. M. El-Zaatari, Y. Fang, S. J. Weigand, F. S. Bates and J. A. Kalow, *Macromolecules*, 2021, **54**, 3972-3986.
- S. Ciarella, F. Sciortino and W. G. Ellenbroek, *Phys. Rev. Lett.*, 2018, **121**, 058003.
- F. I. Altuna, U. Casado, I. E. Dell'Erba, L. Luna, C. E. Hoppe and R. J. J. Williams, *Polym. Chem.*, 2020, **11**, 1337-1347.
- S. Wu and Q. Chen, *Macromolecules*, 2022, **55**, 697-714.
- C. Zhu, Y. Lu, L. Jiang and Y. Yu, *Adv. Funct. Mater.*, 2021, **31**, 2009835.
- Y. Zhai, Z. Wang, K.-S. Kwon, S. Cai, D. J. Lipomi and T. N. Ng, *Adv. Mater.*, 2021, **33**, 2002541.
- D. J. Lipomi, C. Dhong, C. W. Carpenter, N. B. Root and V. S. Ramachandran, *Adv. Funct. Mater.*, 2020, **30**, 1906850.
- M. Giamberjini, E. Amendola and C. Carfagna, *Mol. Cryst. Liq. Cryst. Sci. Technol. Sect. A-Mol. Cryst. Liq. Cryst.*, 1995, **266**, 9-22.
- S. Zhang, Y. Zhang, Y. Wu, Y. Yang, Q. Chen, H. Liang, Y. Wei and Y. Ji, *Chem. Sci.*, 2020, **11**, 7694-7700.

Acknowledgements

This research was supported by the National Natural Science Foundation of China (Nos. 51722303, 21674057, and 21788102).

Keywords: liquid crystal elastomers • vitrimers • actuators

View Article Online

DOI: 10.1039/D2MH00184A

View Article Online
DOI: 10.1039/D3MH00184A

COMMUNICATION

Materials Horizons Accepted Manuscript

Published on 21 February 2023. Downloaded by Tsinghua University on 2/21/2023 3:02:07 AM.